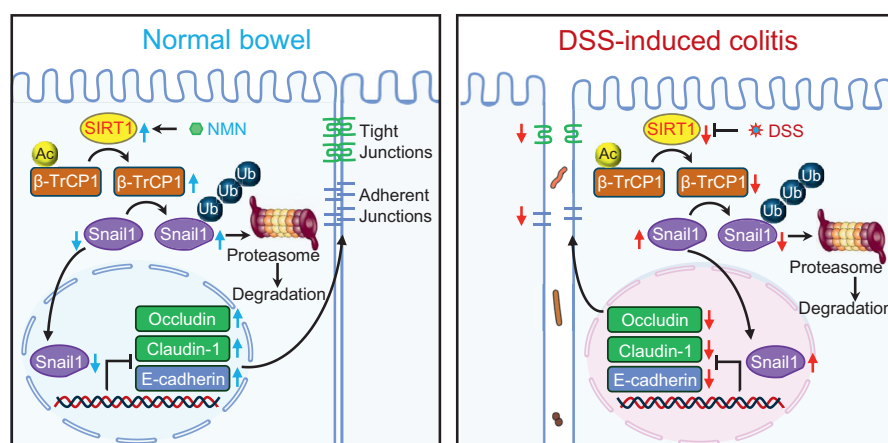


## ORIGINAL RESEARCH

SIRT1 Stabilizes  $\beta$ -TrCP1 to Inhibit Snail1 Expression in Maintaining Intestinal Epithelial Integrity to Alleviate Colitis

Liang Wang,<sup>1,2</sup> Jinsong Li,<sup>2</sup> Mingshan Jiang,<sup>3</sup> Yue Luo,<sup>2</sup> Xiaoke Xu,<sup>2</sup> Juan Li,<sup>2</sup> Yang Pan,<sup>2</sup> Hu Zhang,<sup>3</sup> Zhi-Xiong Jim Xiao,<sup>2</sup> and Yang Wang<sup>2</sup>

<sup>1</sup>Institute of Basic Medicine and Forensic Medicine, North Sichuan Medical College, Nanchong, China; <sup>2</sup>Center of Growth, Metabolism and Aging, Key Laboratory of Bio-Resource and Eco-Environment, Ministry of Education, College of Life Sciences, Sichuan University, Chengdu, China; and <sup>3</sup>Department of Gastroenterology, West China Hospital, Sichuan University, Chengdu, China



cmgh CELLULAR AND MOLECULAR GASTROENTEROLOGY AND HEPATOLOGY

## SUMMARY

DSS-induced mouse colitis is caused by the inhibition of the SIRT1, leading to  $\beta$ -TrCP1 degradation and Snail1 stabilization, resulting in disruption of cell adhesion and tight junction, accompanied by the integrity loss of the epithelial barrier and increased inflammation, which can be alleviated by NMN.

**BACKGROUND & AIMS:** Dysfunction of the intestinal epithelial barrier comprising the junctional complex of tight junctions and adherent junctions leads to increased intestinal permeability, which is a major cause of uncontrolled inflammation related to inflammatory bowel disease (IBD). The NAD<sup>+</sup>-dependent deacetylase SIRT1 is implicated in inflammation and the pathologic process of IBD. We aimed to elucidate the protective role and underlying mechanism of SIRT1 in cell-cell junction and intestinal epithelial integrity.

**METHODS:** The correlation of SIRT1 expression and human IBD was analyzed by GEO or immunohistochemical analyses. BK5.mSIRT1 transgenic mice and wild-type mice were given dextran sodium sulfate (DSS) and the manifestation of colitis-related phenotypes was analyzed. Intestinal permeability was

measured by FITC-dextran and cytokines expression was analyzed by quantitative polymerase chain reaction. The expression of the cell junction-related proteins in DSS-treated or SIRT1-knockdown Caco2 or HCT116 cells was analyzed by Western blotting. The effects of nicotinamide mononucleotide in DSS-induced mice colitis were investigated. Correlations of the SIRT1- $\beta$ -TrCP1-Snail1-Occludin/Claudin-1/E-cadherin pathway with human IBD samples were analyzed.

**RESULTS:** Reduced SIRT1 expression is associated with human IBD specimens. SIRT1 transgenic mice exhibit much-reduced manifestations of DSS-induced colitis. The activation of SIRT1 by nicotinamide mononucleotide bolsters intestinal epithelial barrier function and ameliorates DSS-induced colitis in mice. Mechanistically, DSS downregulates SIRT1 expression, leading to destabilization of  $\beta$ -TrCP1 and upregulation of Snail1, accompanied by reduced expression of E-cadherin, Occludin, and Claudin-1, consequently resulting in increased epithelial permeability and inflammation. The deregulated SIRT1- $\beta$ -TrCP1-Snail1-Occludin/Claudin-1/E-cadherin pathway correlates with human IBD.

**CONCLUSIONS:** SIRT1 is pivotal in maintaining the intestinal epithelial barrier integrity via modulation of the  $\beta$ -TrCP1-Snail1-E-cadherin/Occludin/Claudin-1 pathway. (*Cell Mol Gastroenterol Hepatol* 2024;18:101354; <https://doi.org/10.1016/j.jcmgh.2024.05.002>)

**Keywords:** SIRT1;  $\beta$ -TrCP1; Snail1; Inflammatory Bowel Disease; Intestinal Epithelial Integrity.

Inflammatory bowel disease (IBD), including Crohn's disease and ulcerative colitis (UC), is a chronic, relapsing immune-mediated disease of the intestinal tract, with complex pathophysiology involving genetic, environmental, microbiome, and immunologic factors.<sup>1</sup> Patients with IBD often present with such symptoms as abdominal pain, diarrhea, bloody stools, and loss of appetite, all contributing to a substantial decrease in the patient's quality of life.<sup>2–4</sup> Notably, patients with IBD are at 2- to 3-fold increased risk of developing colorectal cancer,<sup>5,6</sup> which is responsible for approximately 10%–15% of the annual deaths in patients with IBD.<sup>7</sup> Intestinal epithelial cells constitute a continuous physical barrier that is connected by an epithelial junctional complex formed by tight junctions (TJs), adherens junctions (AJs), and desmosomes, which block pathogens and toxic substances.<sup>8,9</sup> Abnormal junctional integrity, especially dysregulation of TJs, is associated with increased intestinal permeability,<sup>10</sup> leading to increased microbial exposure to the mucosal immune system and uncontrolled inflammation.<sup>11–13</sup> The TJ proteins Occludin and Claudin-1 and the AJ protein E-cadherin are significantly decreased in IBD.<sup>14,15</sup> Therefore, identifying new targets and underlying molecular mechanisms that regulate intestinal barrier function may contribute to the prevention and treatment of IBD.

Most IBD mouse models are based either on chemical induction, immune cell transfer, or gene targeting. These mouse models are broadly categorized into defects in epithelial integrity/permeability and defects in the immune system. Intestinal epithelial-cell-specific inhibition of nuclear factor- $\kappa$ B through conditional knockout of NEMO (also called I $\kappa$ B kinase-c [IKKc]) or both IKK1 (IKKa) and IKK2 (IKKb), IKK subunits essential for nuclear factor- $\kappa$ B activation, spontaneously caused severe chronic intestinal inflammation in mice reminiscent of IBD phenotype.<sup>16</sup> A CMV promoter-driven STAT4 transgenic mice expressed strikingly increased nuclear STAT4 levels in lamina propria CD4+ T lymphocytes and developed chronic transmural colitis characterized by infiltrates of mainly CD4+ T lymphocytes leading to chronic intestinal inflammation.<sup>16</sup> Dextran sulfate sodium (DSS)-induced colitis mice are the most commonly used IBD model because they share many manifestations and pathologic characteristics with human disease.<sup>17</sup>

SIRT1, a member of the mammalian sirtuins family of proteins that are homologous to yeast silent information regulator 2 (*Sir2*), is an NAD<sup>+</sup>-dependent protein deacetylase and plays an important role in regulating multiple biologic processes, such as cell senescence,<sup>18,19</sup> energy metabolism,<sup>20</sup> oxidative stress,<sup>21–23</sup> inflammation,<sup>23,24</sup> mitochondrial biogenesis,<sup>25</sup> apoptosis,<sup>26</sup> and autophagy.<sup>27,28</sup> Recent investigations have increasingly highlighted the crucial involvement of SIRT1 in the pathogenesis of IBD.<sup>29,30</sup> Loss of SIRT1 in the intestinal epithelium contributes to enhancing intestinal inflammation and increased susceptibility to colitis.<sup>31</sup> SIRT1 activator SRT1720 decreases the disease activity index, inflammatory cytokine

levels, and colon histologic score in mice with DSS-induced colitis, whereas nicotinamide (SIRT1 inhibitor) administration exerts the opposite effects.<sup>32</sup> Resveratrol, an activator of SIRT1, suppresses the activation of the NLRP3 inflammasome and alleviates bowel inflammation in mice with radiation-induced IBD.<sup>33</sup> The administration of a SIRT1 inhibitor, EX-527, increased the disease severity and infiltration of CD3+ T cells in the mouse colon.<sup>34</sup> Cay10591, a SIRT1 agonist, decreased the generation of proinflammatory cytokines.<sup>34</sup> These results suggest that SIRT1 plays a vital role in epithelial integrity and that dysfunction of SIRT1 is closely linked to IBD. However, how SIRT1 regulates intestinal epithelial junction remains unclear.

Snail1 is a transcriptional repressor that negatively regulates the expression of various target genes, including Occludin, Claudin-1, and E-cadherin, by binding to the E-box motif in the promoter of them and plays a crucial role in various biologic processes, such as embryonic development, epithelial-mesenchymal transition, cell survival, and cellular stemness.<sup>35–39</sup> Notably, it has been reported that Snail1 is significantly increased in IBD.<sup>40</sup> However, the regulation of Snail1 in IBD remains unclear.


In this study, our findings delineate that overexpression of SIRT1 fortifies the intestinal epithelial barrier against DSS, substantially mitigating DSS-induced colitis in mice. We further demonstrate that SIRT1 maintains the junctional integrity of intestinal epithelial cells. Significantly, we provide novel insights showing that SIRT1 governs the expression of TJ and AJ proteins through the  $\beta$ -TrCP1-Snail1 pathway. Moreover, our data indicate that nicotinamide mononucleotide (NMN), a precursor of NAD<sup>+</sup>, notably ameliorates DSS-induced colitis in mice by potentiating the SIRT1 signaling pathway.

## Results

### *Ectopic Expression of SIRT1 Attenuates DSS-Induced Colitis in Mice*

Given the reported significance of sirtuins in intestinal disease,<sup>41</sup> we investigated the alterations of sirtuins in UC. Analyses of the GSE9452 dataset revealed a significant reduction in SIRT1 mRNA expression in colonic tissue from patients with UC, whereas the expression levels of other sirtuins remained statistically unchanged (Figure 1A). Furthermore, a diminished expression of SIRT1 was detected in the colonic epithelium of patients with UC (Figure 1B). These findings suggest that downregulation of SIRT1 is associated with the pathogenesis of human UC.

**Abbreviations used in this paper:** AJ, adherens junction; DMEM, Dulbecco's modified Eagle's medium; DSS, dextran sodium sulfate; IBD, inflammatory bowel disease; NMN, nicotinamide mononucleotide; PBS, phosphate-buffered saline; qPCR, quantitative polymerase chain reaction; TJ, tight junctions; UC, ulcerative colitis.

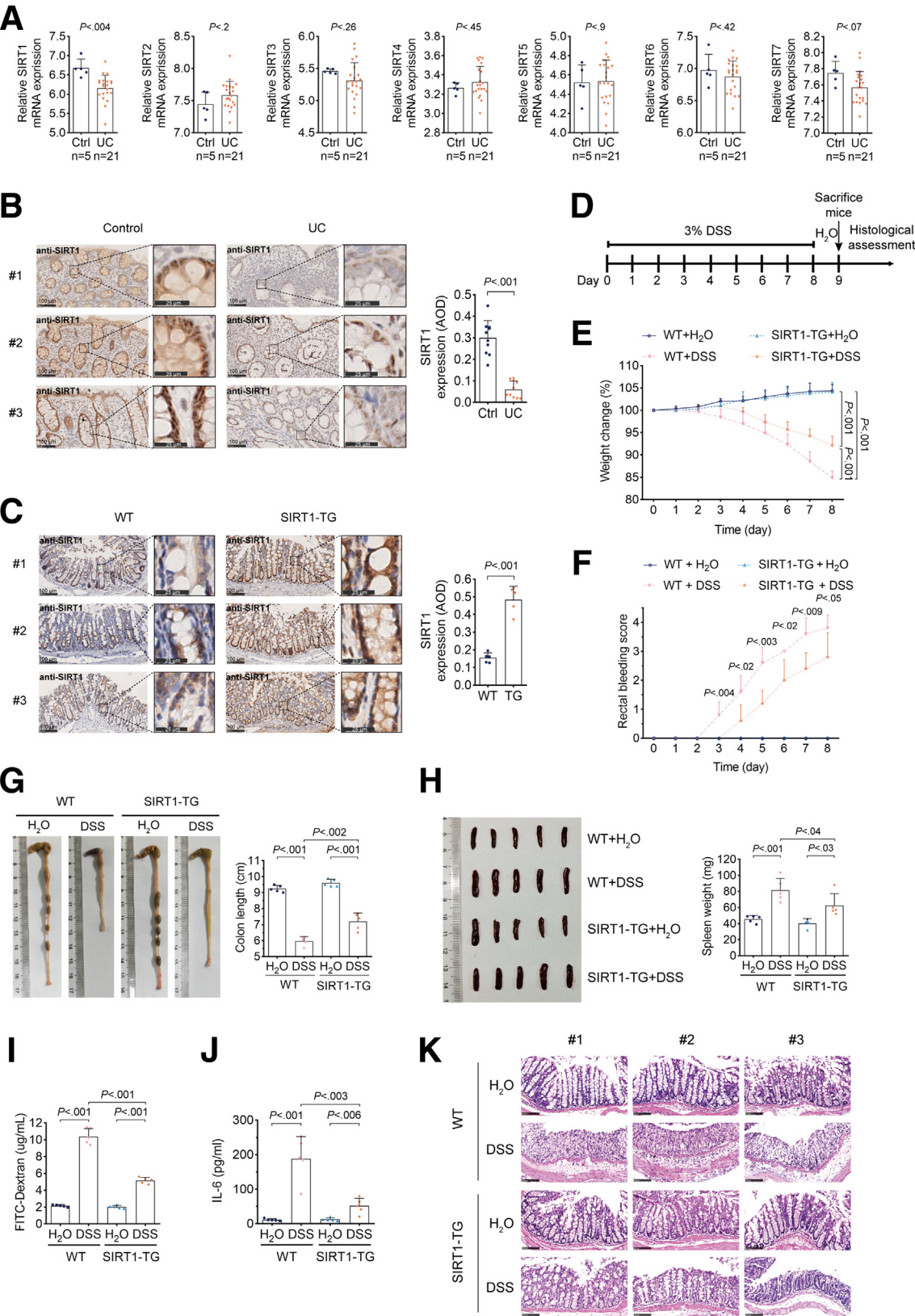
 Most current article

© 2024 The Authors. Published by Elsevier Inc. on behalf of the AGA Institute. This is an open access article under the CC BY-NC-ND license (<http://creativecommons.org/licenses/by-nc-nd/4.0/>).

2352-345X

<https://doi.org/10.1016/j.jcmgh.2024.05.002>

To investigate the causal role of SIRT1 in the pathogenesis of human UC, we designed and constructed transgenic mice, in which the murine *Sirt1* gene is under the control of the bovine keratin 5 promoter (BK5) to drive *Sirt1* expression in epithelial cells in C57BL/6 mice, termed SIRT1-TG mice. As shown in Figure 1C, increased SIRT1





protein expression was readily detected in intestinal epithelial cells.

We then induced acute colitis in wild-type and SIRT1-TG mice by supplementing of 3% DSS in drinking water for 8 days (Figure 1D). As shown in Figure 1, compared with wild-type mice, the SIRT1-TG mice manifested a substantial attenuation in clinical indications of colitis, encompassing reduced weight loss (Figure 1E), diminished bloody stools (Figure 1F), less pronounced colon shortening (Figure 1G), and a lesser increase in spleen size (Figure 1H). Consistent with these findings, the content of FD4 in serum from SIRT1-TG mice was significantly decreased after DSS administration (Figure 1I), indicating that the intestinal permeability of SIRT1-TG mice was lower than wild-type mice after DSS administration. Moreover, the proinflammatory cytokine interleukin-6 levels in the serum of SIRT1-TG mice was significantly decreased (Figure 1J). Histologic examination showed less colonic mucosal morphologic damage induced by DSS in SIRT1-TG mice compared with wild-type mice (Figure 1K). These findings suggest that overexpression of SIRT1 attenuates the severity of DSS-induced colitis in mice.

### ***SIRT1 Mitigates DSS-Induced Cell-Cell Junction Dysfunction by Diminishing the Stability of Snail1***

TJ and AJ play crucial roles in the intestinal barrier, governing the regulation of epithelial permeability.<sup>10,14</sup> Notably, quantitative polymerase chain reaction (qPCR) analyses showed that the mRNA levels of genes encoding E-cadherin and Occludin, 2 critical cell-cell junction-associated proteins, were markedly reduced in the colon tissues of patients with UC (Figure 2A). Furthermore, on DSS treatment, human colon carcinoma Caco2 cells exhibited reduction in SIRT1 protein levels, concomitant with a decrease in the levels of cell-cell junction-associated proteins, including E-cadherin, Occludin, and Claudin-1, accompanied by an increase in Snail1 protein expression (Figure 2B). By contrast, ectopic expression of SIRT1 effectively reversed DSS-induced alteration of protein expression of Snail1, E-cadherin, Occludin, and Claudin-1 (Figure 2C). Aligning with these findings, the ectopic expression of SIRT1 markedly reversed the DSS-induced increase of intercellular permeability of FD4 (Figure 2D). Together, these results indicate that SIRT1 plays an important role in modulation of

expression of cell adhesion proteins, which are associated with human IBD and DSS-induced mouse colitis.

Snail1 has been shown as a critical transcription factor regulating the expression of E-cadherin, Occludin, and Claudin-1.<sup>36</sup> We therefore investigated the role of Snail1 in the protective effects of SIRT1 against dysfunction of DSS-induced cell-cell junctions. As shown in Figure 2E, the knockdown of Snail1 significantly impeded the DSS-induced downregulation of E-cadherin and Claudin-1.

Next, we investigated the underlying mechanisms by which DSS upregulates Snail1 expression. DSS treatment led to a reduction in Snail1 ubiquitination (Figure 2F), concomitant with prolonged half-life of Snail1 protein (Figure 2G). Together with the observation in Figure 2C that ectopic expression of SIRT1 effectively reversed DSS-induced alteration of Snail1 protein expression, these results suggest that DSS inhibits SIRT1 expression, which in turn facilitates Snail1 protein ubiquitination and degradation, thereby impacting cell-cell junction.

### ***SIRT1 Deacetylates and Stabilizes $\beta$ -TrCP1 Protein to Downregulate Snail1***

It is well-documented that the stability of the Snail1 protein is modulated by certain E3 ligases, including  $\beta$ -TrCP1 and FBXL14.<sup>42</sup> We therefore investigated whether SIRT1 promotes Snail1 degradation by modulating its specific E3 ligases. As shown in Figure 3A, the knockdown of SIRT1 led to the downregulation of  $\beta$ -TrCP1 but not FBXL14, accompanied by the upregulation of Snail1 protein expression. Notably, in addition to the readily detectable  $\beta$ -TrCP1-Snail1 protein complex formation in vivo, in keeping with a previous report<sup>43</sup> (Figure 3B), ectopic expression of  $\beta$ -TrCP1 effectively blocked SIRT1 silence-induced upregulation of Snail1, accompanied by restored expression of E-cadherin, Occludin and Claudin-1 (Figure 3C).

We next examined how DSS affected the expression of cell-cell adhesion proteins. As shown in Figure 3D, DSS treatment led to the downregulation of SIRT1, concomitant with the downregulation of  $\beta$ -TrCP1, whereas the expression of FBXL14 was not significantly changed, suggesting that  $\beta$ -TrCP1 plays a role in DSS-induced upregulation of Snail1. Similar effects of DSS on the expression of SIRT1,  $\beta$ -TrCP1, Snail1, E-cadherin, Occludin, or Claudin-1 were observed in HCT116 human colon cancer cells (Figure 3E). Ectopic expression of SIRT1 upregulated  $\beta$ -TrCP1 and

**Figure 1. (See previous page). Overexpression of SIRT1 attenuates DSS-induced colitis in mice.** (A and B) Reduced SIRT1 expression in the colon epithelium is associated with human IBD patients. (A) The expression of SIRT1-SIRT7 mRNAs in colons derived from human UC patients and control subjects was analyzed using the GEO GSE9452 dataset. (B) Representative immunohistochemistry staining of SIRT1 in the colonic epithelium of human non-IBD (n = 23) and IBD patients (n = 16). (C–K) Overexpression of SIRT1 attenuates DSS-induced colitis in mice. (C) Representative immunohistochemistry staining of SIRT1 in the colonic epithelium of wild-type (WT) or SIRT1-TG mice (n = 5/group). (D) Schematic overview of the experimental design. (E–H) Four-month-old SIRT1-TG mice (n = 5) or age-matched wild-type mice (n = 5) were fed with 3% DSS in drinking water for 8 days as depicted in D. Body weights (E), rectal bleeding scores (F), colon appearance and length (G), and spleen appearance and weights (H) were presented. (I–K) Mice (n = 5/group) pretreated with 3% DSS in drinking water for 8 days then fasted for 8 hours followed by garaging with FITC-Dextran (FD4) (0.6 mg/g in PBS). Plasma samples were collected 4 hours later and subjected either to measurement of fluorescence intensity (I) or to enzyme-linked immunosorbent assay for cytokine interleukin (IL)-6 (J). Representative H/E-staining images of colon tissues were shown (K). Data were presented as mean  $\pm$  standard error of the mean. Comparisons were performed with 2-tailed Student test (A) or 2-way analysis of variance with Tukey test (E–J).

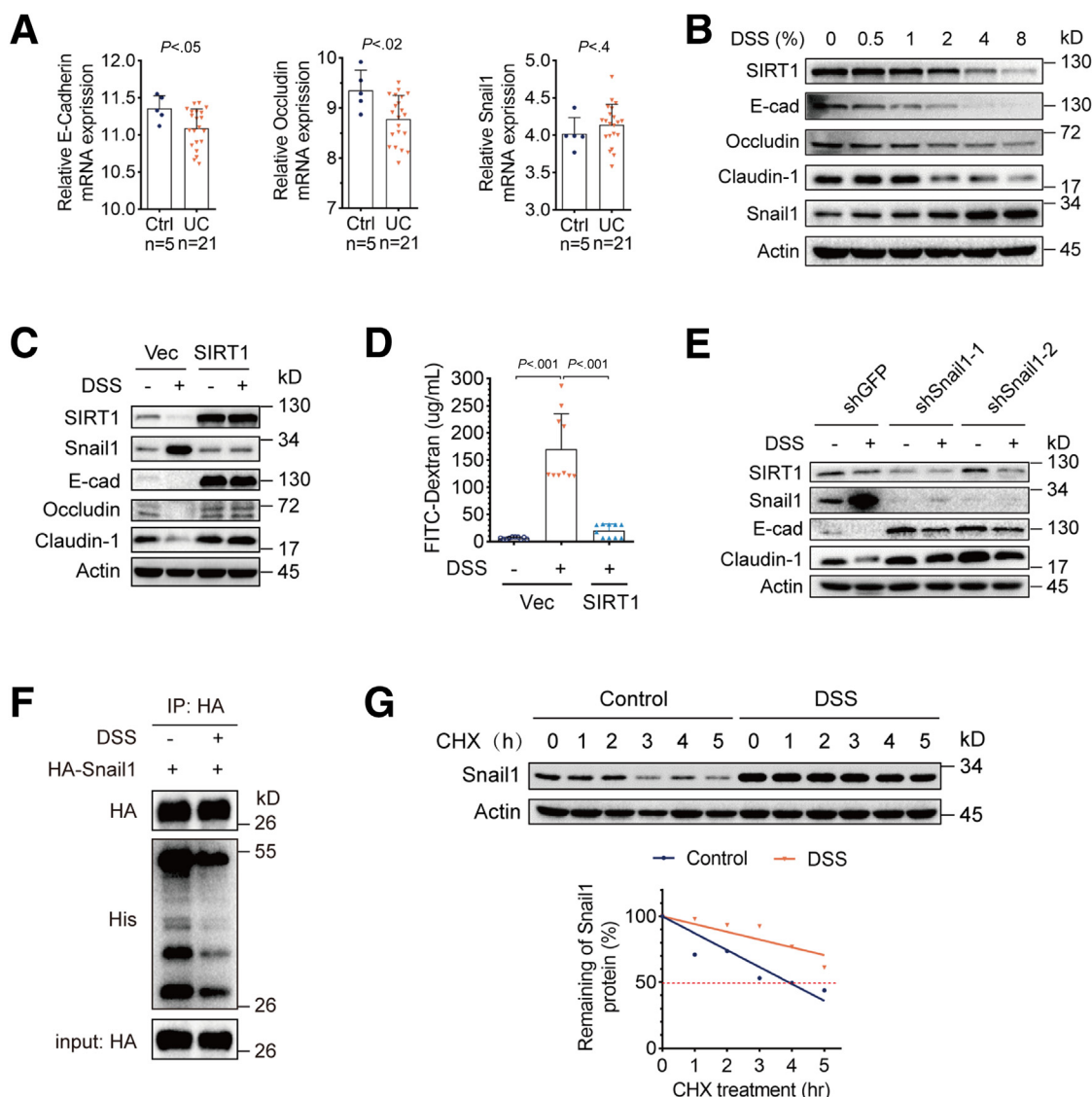
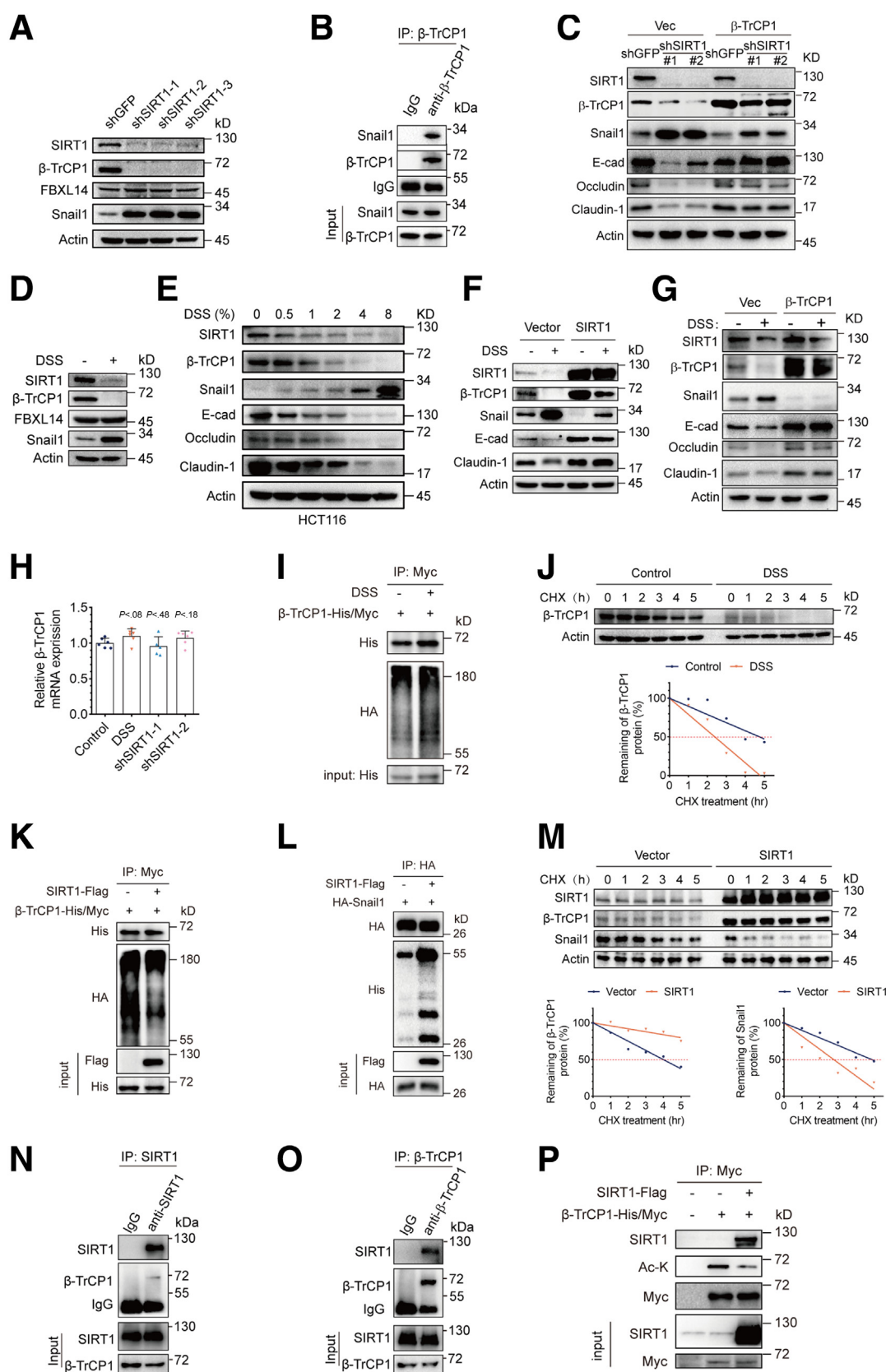


**Figure 2. DSS inhibits SIRT1 expression to promote Snail1 protein stabilization resulting in the downregulation of cell adhesion proteins and increased intercellular permeability.** (A) Analyses of the GEO GSE9452 dataset. Notice that significantly reduced mRNA expression of E-cadherin and Occludin, but not Snail1 in colons from human UC patients. (B) The human colon cancer Caco2 cells were treated with an increasing dose of DSS for 8 hours. Whole-cell lysates were subjected to Western blotting for expression of various proteins as indicated. (C) Caco2 cells stably overexpressing SIRT1 were treated with 4% DSS for 8 hours. Whole-cell lysates were subjected to Western blotting. (D) To measure intercellular permeability, Caco2 cells stably overexpressing SIRT1 were treated with 4% DSS for 8 hours before analyzing FD4 flux. (E) Caco2 cells stably expressing shGFP, shSnail1-1, and shSnail1-2 treated in the presence or absence of DSS (4%; 8 hours) were subjected to Western blotting analyses for several adhesion proteins as indicated. (F) To examine the effects of DSS on ubiquitination of Snail1, 293FT cells were cotransfected with the relevant expression plasmids for 48 hours, followed by treatment with 4% DSS for 12 hours. Before harvesting, cells underwent treatment with 20  $\mu$ M MG132 for 6 hours. Ubiquitination of Snail1 was examined by denature-IP-western analyses. (G) The Snail1 protein half-lives were measured by CHX assays in Caco2 cells treated with or without DSS. Data derived from 2 independent experiments at least in triplicates were presented as mean  $\pm$  standard error of the mean. Comparisons were performed with a 2-tailed Student test (A) or 2-way analysis of variance with Tukey test (D).

reversed the effects of DSS-induced expression of either  $\beta$ -TrCP1, Snail1, E-cadherin, or Claudin-1 (Figure 3F). Similarly, ectopic expression of  $\beta$ -TrCP1 also reversed the effects of DSS-induced expression of either Snail1, E-cadherin, Occludin, or Claudin-1 (Figure 3G).

Together, these results indicate that SIRT1 positively regulates the expression of  $\beta$ -TrCP1 thereby promoting Snail1 degradation, and that DSS disrupts the cell-cell junction by impacting the axis involved in SIRT1- $\beta$ -TrCP1-Snail1-E-cadherin/occludin/Claudin-1.



We further explored the molecular mechanisms by which SIRT1 regulates  $\beta$ -TrCP1. Our results showed that there were no significant changes in steady-state mRNA levels of  $\beta$ -TrCP1 on SIRT1 knockdown or DSS treatment (Figure 3H), suggesting that SIRT1 likely regulates  $\beta$ -TrCP1 protein turnover. Indeed, DSS treatment led to an augmentation in  $\beta$ -TrCP1 ubiquitination (Figure 3I), accompanied by shortened half-life of  $\beta$ -TrCP1 in Caco2 cells (Figure 3J). Conversely, SIRT1 overexpression markedly reduced ubiquitination of  $\beta$ -TrCP1 and increased ubiquitination of Snail1 (Figure 3K and L), leading to the enhanced the stability of  $\beta$ -TrCP1 and reduced the stability of Snail1 (Figure 3M). Notably, SIRT1 could form stable endogenous protein complexes with  $\beta$ -TrCP1 (Figure 3N and O). Furthermore, ectopic expression of SIRT1 could downregulate the acetylation level of the  $\beta$ -TrCP1 protein (Figure 3P), in keeping with a previous study.<sup>44</sup> Together, these results indicate that SIRT1 facilitates deacetylation and stabilization of the  $\beta$ -TrCP1, which in turn promotes Snail1 protein degradation.

### ***DSS Modulates the SIRT1- $\beta$ -TrCP1-Snail1 Axis to Impact the Expression of TJ Proteins in Colonic Organoids***

To elucidate the role of the SIRT1- $\beta$ -TrCP1-Snail1 axis in colitis pathogenesis, we used colonic organoids as our experimental model. As shown in Figure 4A and B, lentiviral-based knockdown of SIRT1 led to a significant reduction of  $\beta$ -TrCP1 expression and an upregulated Snail1 expression, accompanied by the downregulation of Occludin and Claudin-1, 2 critical TJ proteins. Furthermore, colonic organoids treated with DSS exhibited a marked reduction in SIRT1 expression, concomitant with similar changes in the signaling pathways observed by specific knockdown of SIRT1. Importantly, in the rescuing experiments, either overexpressing  $\beta$ -TrCP1 or knocking down Snail1 led to significantly restored expression of Occludin and Claudin-1, highlighting the potential regulatory mechanisms at play in colitis. Notably, the knockdown of SIRT1 significantly inhibited the growth of colonic organoids, suggesting a vital

role of SIRT1 in regulating stemness and proliferation in the colon (Figure 4C).

### ***NMN Ameliorates DSS-Induced Colitis in Mice Via Activating the SIRT1- $\beta$ -TrCP1 Axis***

Next, we explored the means of interference of the SIRT1- $\beta$ -TrCP1 axis to reduce DSS-induced colitis in mice. Thus, we turned into the small molecule activators for SIRT1. NMN, a precursor of NAD<sup>+</sup>, increases activation of SIRT1 by promoting NAD<sup>+</sup> biosynthesis.<sup>45,46</sup> Previous studies have illustrated the potential therapeutic effects of NMN in various diseases, such as diabetes, ischemia-reperfusion injury, heart failure, Alzheimer disease, and retinal degeneration.<sup>47</sup> However, the role and underlying mechanisms of NMN in human IBD remain elusive.

Caco2 cells were pretreated with an increasing concentration or time dose of NMN before the exposure of 4% DSS for 8 hours. Our analyses showed that, in a dose- and time-dependent manner, NMN could well mitigate the DSS-induced downregulation of SIRT1 and  $\beta$ -TrCP1, accompanied by increased expression of E-cadherin, Occludin, and Claudin-1 (Figure 5A and B). Notably, NMN not only significantly recovered the SIRT1 deacetylase activity suppressed by DSS and elevated SIRT1 mRNA levels (Figure 5C and D), but also it significantly attenuated the DSS-induced transepithelial permeability of FITC-Dextran (Figure 5E). Importantly, although NMN could markedly reverse DSS-mediated effects on the expression of  $\beta$ -TrCP1, Snail1, E-cadherin, Occludin, and Claudin-1, NMN could not exhibit any effects in SIRT1-silenced Caco2 cells (Figure 5F).

To assess the potential therapeutic effect of NMN on colitis, DSS-treated mice were intraperitoneal injected daily with NMN (0.3 mg/g). Compared with the normal mice (n = 5), mice treated with NMN (n = 5) exhibited much reduced clinical manifestation of colitis, including less weight loss (Figure 5G), reduced bloody stool (Figure 5H), lesser colon length shorting (Figure 5I), reduced spleen size enlargement (Figure 5J), reduced intestinal permeability (Figure 5K), and less colonic mucosal morphologic damage (Figure 5L). Moreover, immunohistochemistry analysis showed that a

**Figure 3. (See previous page). SIRT1 deacetylates and stabilizes  $\beta$ -TrCP1 protein to downregulate Snail1.** (A) Caco2 cells stably expressing shRNAs against SIRT1 were subjected to Western blotting. (B) Caco2 cell lysates were subjected to immunoprecipitation (IP) with anti- $\beta$ -TrCP1, using normal mouse or rabbit IgG as a control, followed by Western blot analyses. (C) Caco2 cells stably coexpressing  $\beta$ -TrCP1 and shRNAs against SIRT1 were subjected to Western blotting. (D) Caco2 cells treated with or without DSS were subjected to Western blotting. (E) HCT116 cells were treated with 4% DSS for 8 hours and the whole cell lysates were subjected to Western blotting. (F) Caco2 cells stably overexpressing SIRT1 were treated with 4% DSS for 8 hours. Whole-cell lysates were subjected to Western blotting. (G) Caco2 cells stably overexpressing  $\beta$ -TrCP1 were treated with 4% DSS for 8 hours. Whole-cell lysates were subjected to Western blotting. (H) Caco2 cells pretreated with 4% DSS for 8 hours or stably expressing shRNAs against SIRT1 were subjected to qPCR analyses for  $\beta$ -TrCP1. (I) To examine the effects of DSS on ubiquitination of  $\beta$ -TrCP1, 293FT cells were cotransfected with the relevant expression plasmids for 48 hours, followed by treatment with 4% DSS for 12 hours. Before harvesting, cells underwent treatment with 20  $\mu$ M MG132 for 6 hours. Ubiquitination of  $\beta$ -TrCP1 was examined by denature-IP-western analyses. (J) The  $\beta$ -TrCP1 protein half-lives were measured by CHX assays in Caco2 cells pretreated with 4% DSS for 8 hours. (K and L) To examine the effects of SIRT1 on ubiquitination of  $\beta$ -TrCP1 and Snail1, 293FT cells were cotransfected with indicated expressing plasmids. Cells were treated with 20  $\mu$ M MG132 for 6 hours before collection. Ubiquitination of Snail1 was examined by denature-IP-western analyses. (M) The  $\beta$ -TrCP1 and Snail1 protein half-lives were measured by CHX assays in Caco2 cells stably overexpressing SIRT1. (N and O) Caco2 cell lysates were subjected to IP with anti-SIRT1 (H) or anti- $\beta$ -TrCP1 (I), using normal mouse or rabbit IgG as a control, followed by Western blot analyses. (P) HEK-293T cells cotransfected with His/Myc- $\beta$ -TrCP1 and Flag-SIRT1 were subjected to IP and Western blotting analyses.



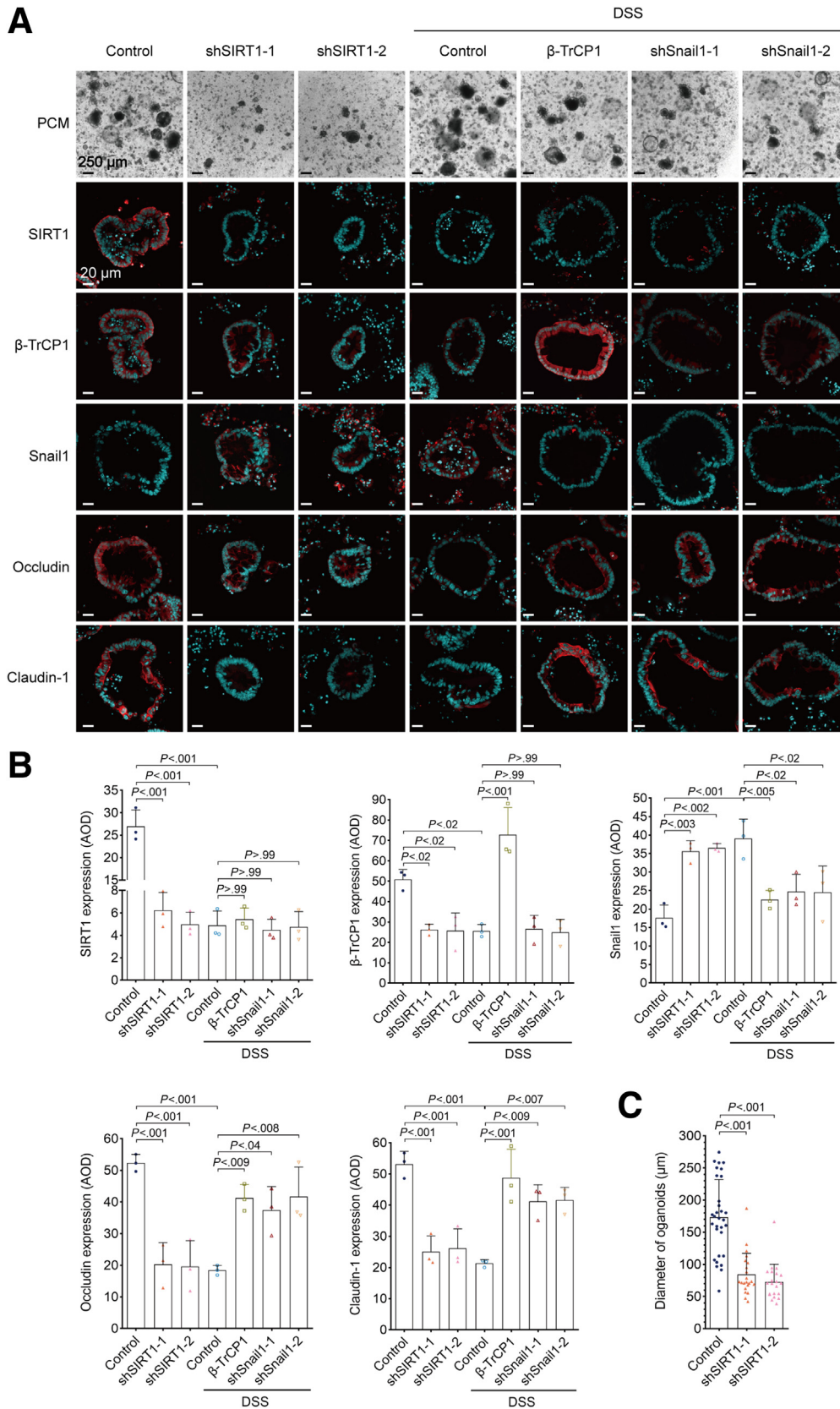


**Figure 4.** The SIRT1- $\beta$ -TrCP1-Snail1 axis preserves cell tight junction in murine colon organoids. (A–C) Colonic crypts derived from 2-month-old C57/BL6 male mice were infected with a recombinant lentivirus expressing  $\beta$ -TrCP1 or shRNA specific for SIRT1 or Snail1, which were then subjected to colonic organoid growth in vitro. Eight days after the virus infection, organoids were treated with or without 4% DSS for 6 hours. Subsequent analysis involved phase contrast microscopy (PCM) and immunofluorescent staining (A). The expression of the relevant proteins was quantified by average optical density (B), as described in the [Materials and Methods](#). The diameters of colonic organoids infected with a recombinant lentivirus expressing shRNA specific for SIRT1 at day 8 were quantified. Control, n = 31 organoids; shSIRT1-1, n = 22 organoids; shSIRT1-2, n = 21 organoids (C). Experiments were performed 3 times independently. Data were means  $\pm$  standard error of the mean. Statistical analyses were performed using 2-way analysis of variance with Tukey test. Scale bar = 250 or 20  $\mu$ m as indicated.

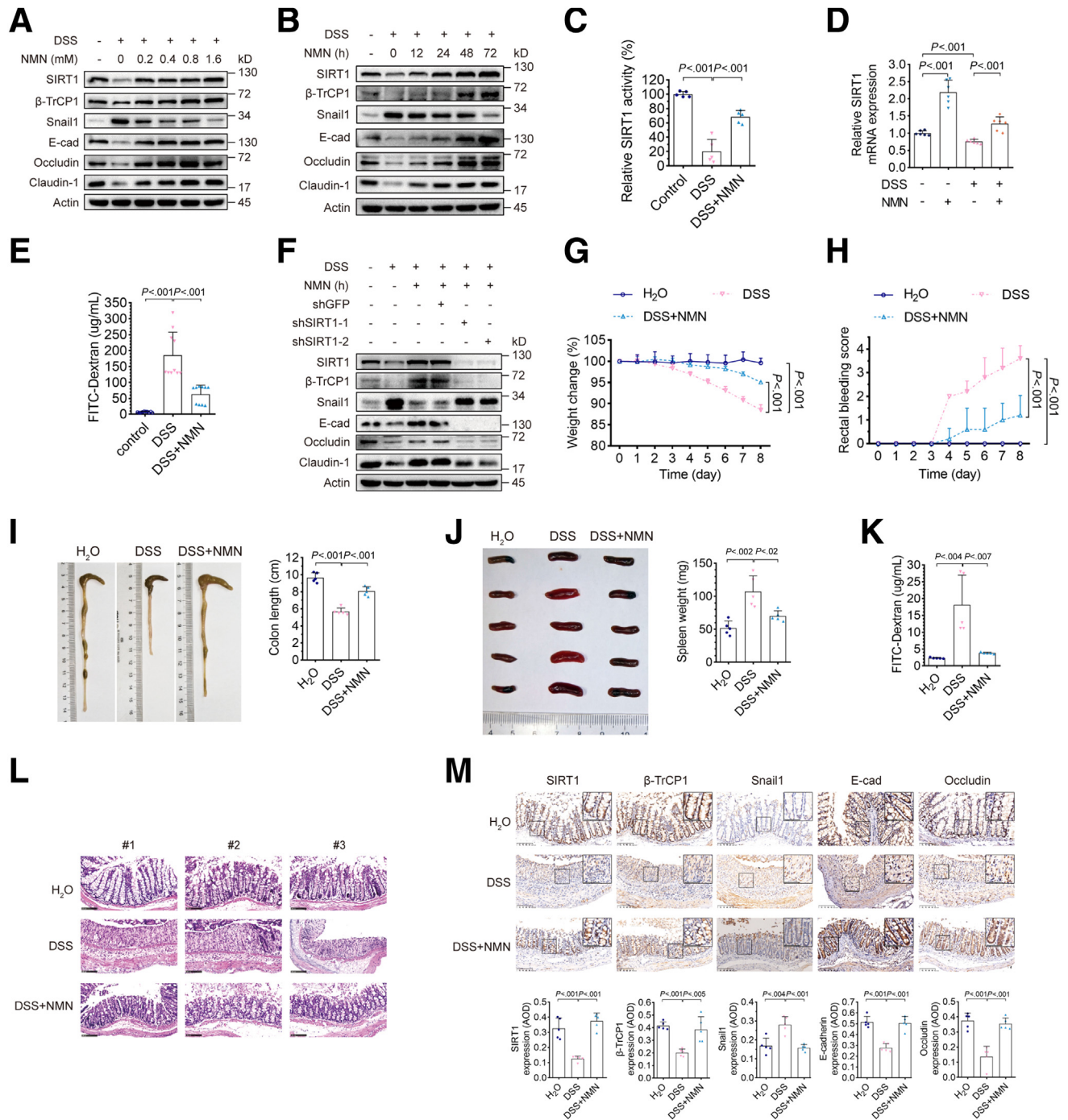


substantial restoration of DSS-suppressed expression of SIRT1,  $\beta$ -TrCP1, E-cadherin, and Occludin, concomitant with reduction of DSS-induced increase of Snail1 (Figure 5M). Taken together, these results indicate that NMN ameliorates DSS-induced colitis in mice via activating SIRT1.

*The SIRT1- $\beta$ -TrCP1-Snail1 Signaling Pathway Plays an Important Role in Human IBD*

To further investigate the clinical correlation between the SIRT1- $\beta$ -TrCP1-Snail1 axis and IBD, we examined the

expression of relevant genes in human IBD samples. Our results showed that the mRNA levels of either SIRT1, E-cadherin, or Occludin were significantly decreased, whereas there were no significant changes in mRNA levels of  $\beta$ -TrCP1 and Snail1 in human UC (Figure 6A). Moreover, immunohistochemistry analyses showed that the protein levels of SIRT1,  $\beta$ -TrCP1, E-cadherin, Occludin, and Claudin-1 were significantly decreased, whereas Snail1 protein levels were significantly increased in colonic tissues from IBD patients (Figure 6B and C). Further correlation analyses showed a relationship on the



protein expression between SIRT1 and the  $\beta$ -TrCP1-Snail1-Occludin/Claudin-1/E-cadherin in human IBD (Figure 6D).

## Discussion

IBD is marked by the dysfunctional intestinal epithelial barrier, in which the integrity of epithelial structures is disrupted by abnormal TJs, AJs, or desmosomes, resulting in the diffusion of pathogens and toxic substances across the barrier and uncontrolled inflammation.<sup>8,9</sup> In this study, we showed that SIRT1 plays a pivotal role in maintaining the integrity of the epithelial structures through modulation of the expression of proteins involved in TJ and AJ.

SIRT1 is implicated in the pathophysiology of IBD development. However, the precise role of SIRT1 in IBD is still under debate. Clinical evidence indicates that there is a significant downregulation of mRNA and protein expression of SIRT1 in the colonic biopsies from Crohn's disease and UC, notably, the downregulation of SIRT1 is mainly restricted to the areas of active inflammation,<sup>30</sup> suggesting that SIRT1 plays a critical role in the inflammation associated with colitis. The intestinal-specific *Sirt1* deletion promotes antibacterial defense and protects the mice from the development of colitis.<sup>48</sup>

We focused on the role of SIRT1 in the integrity of intestinal epithelial structure and function. It has been reported that the reduced expression of SIRT1 in epithelial crypt cells is observed in IBD samples.<sup>49</sup> In DSS-induced colitis of mice models, knockout of SIRT1 in epithelial cells exacerbates DSS-induced manifestation of colitis including rectal bleeding, bloody diarrhea, and colonic shortening,<sup>31</sup> the molecular mechanisms of which remain unclear. Our investigation revealed that the elevation of SIRT1 expression in epithelial cells or activation of SIRT1 by NMN significantly ameliorates the severity of DSS-induced colitis in mice, in keeping with previous reports that activation of SIRT1 by resveratrol or SIRT1720 reduces DSS-induced colitis.<sup>49,50</sup>

One important finding of this study is that SIRT1 plays a pivotal role in the regulation of AJ protein E-cadherin and the TJ proteins, Occludin and Claudin-1. Activation of SIRT1

facilitates  $\beta$ -TrCP1 protein deacetylation and stabilization, resulting in Snail1 degradation,<sup>44</sup> and consequently leading to upregulated expression of E-cadherin, Occludin, and Claudin-1. DSS inhibits the SIRT1 gene transcription, resulting in the dysfunction of the SIRT1- $\beta$ -TrCP1-Snail1 signaling and the reduction of E-cadherin, Occludin, and Claudin-1 protein expression, thereby disrupting the intestinal barrier integrity, and promoting inflammation and colitis. This finding is consistent with previous studies showing that DSS can induce downregulation of cell adhesion proteins.<sup>51–54</sup>

Snail1 is an orchestrator of epithelial-mesenchymal transition, governing the repression of epithelial markers while facilitating the expression of mesenchymal markers.<sup>35,36,55</sup> In this study, we demonstrate that SIRT1 plays a central role in maintaining the integrity of the intestinal epithelial barrier as evidenced by our observation that DSS suppresses SIRT1 expression and dramatically upregulates Snail1. Importantly, elevated Snail1 expression and reduced expression of E-cadherin, Occludin, and Claudin-1 protein expression were observed in UC and patients with Crohn's disease, consistent with previous reports.<sup>40</sup>

The role of  $\beta$ -TrCP1 involvement in intestinal barrier function and IBD pathogenesis has remained largely unexplored. Our findings reveal a marked downregulation of  $\beta$ -TrCP1 in patients with IBD and DSS-induced colitis mice. It is well documented that  $\beta$ -TrCP1 is an E3 ligase of Snail1,<sup>56</sup> yet the precise mechanisms are seemingly contradictory. One study indicates that SIRT1 deacetylates  $\beta$ -TrCP1 at K304 and K466 leading to the increase of  $\beta$ -TrCP1 stability,<sup>44</sup> whereas another study shows that SIRT1 inhibits  $\beta$ -TrCP1 accumulation by facilitating its degradation.<sup>57</sup> Our research demonstrates that SIRT1 promotes deacetylation and stabilization of  $\beta$ -TrCP1. Collectively, this study offers strong evidence of the protective role of the SIRT1- $\beta$ -TrCP1 axis in maintaining the integrity of the intestinal epithelial barrier.

Presently, the therapeutic mainstay for IBD consists of immunosuppressants and anti-inflammatory agents, both bearing varying degrees of toxicities and side effects,<sup>58–61</sup>

**Figure 5. (See previous page). NMN ameliorates DSS-induced colitis in mice by activating SIRT1.** (A) Caco2 cells were pretreated for 48 hours with an increasing dose of NMN before DSS treatment (4% for 8 hours). Cell lysates were subjected to Western blotting. (B) Caco2 cells were pretreated with 0.8 NMN for an indicated time interval before DSS (4% for 8 hours) treatment. Cell lysates were subjected to Western blotting. (C) Caco2 cells were pretreated for 48 hours with 0.8 mM NMN before DSS treatment (4% for 8 hours). Equal amounts of immunoprecipitated SIRT1 proteins were subjected to examine deacetylation activity using Fluor-de-Lys SIRT1 fluorometric assay kit and the relative deacetylase activities were presented. (D) Caco2 cells were pretreated with 0.8 NMN for 48 hours before DSS treatment followed by qPCR analyses for SIRT1 expression. Data were presented as mean  $\pm$  standard error of the mean. Comparisons were performed with 2-way analysis of variance with Tukey test. (E) Caco2 cells were pretreated with 0.8 mM NMN for 48 hours before DSS (4% for 8 hours) treatment followed by measurements of intercellular permeability. (F) To examine the role of SIRT1 in the action of NMN, Caco2 cells stably expressing SIRT1 shRNAs were pretreated with 0.8 mM NMN for 48 hours before DSS (4% for 8 hours) treatment followed by Western blotting. (G–M) C57BL/6 mice (n = 5/group) were fed with 3% DSS in drinking water. The NMN groups were administered daily with NMN (0.3 mg/g bodyweight) by intraperitoneal injection. Body weight changes (G) and feces occult blood scores (H) of each mouse were measured daily during DSS treatment. Colon length (I) and spleen weight (J) were measured. (K) All mice were fasted for 8 hours and then garaged with FD4. Plasma samples were subjected to the measurement of fluorescence intensity. (L) Representative hematoxylin and eosin staining images of colon tissues were shown. (M) The expression of SIRT1,  $\beta$ -TrCP1, Snail1, E-cadherin, or Occludin in the colonic epithelium of mice was examined by immunohistochemistry (Scale bar = 100  $\mu$ m; the enlarged pictures: scale bar = 50  $\mu$ m). Data were presented as mean  $\pm$  standard error of the mean. Comparisons were performed with 2-way analysis of variance with Tukey test (C–E, G–M). (n = 5/group).



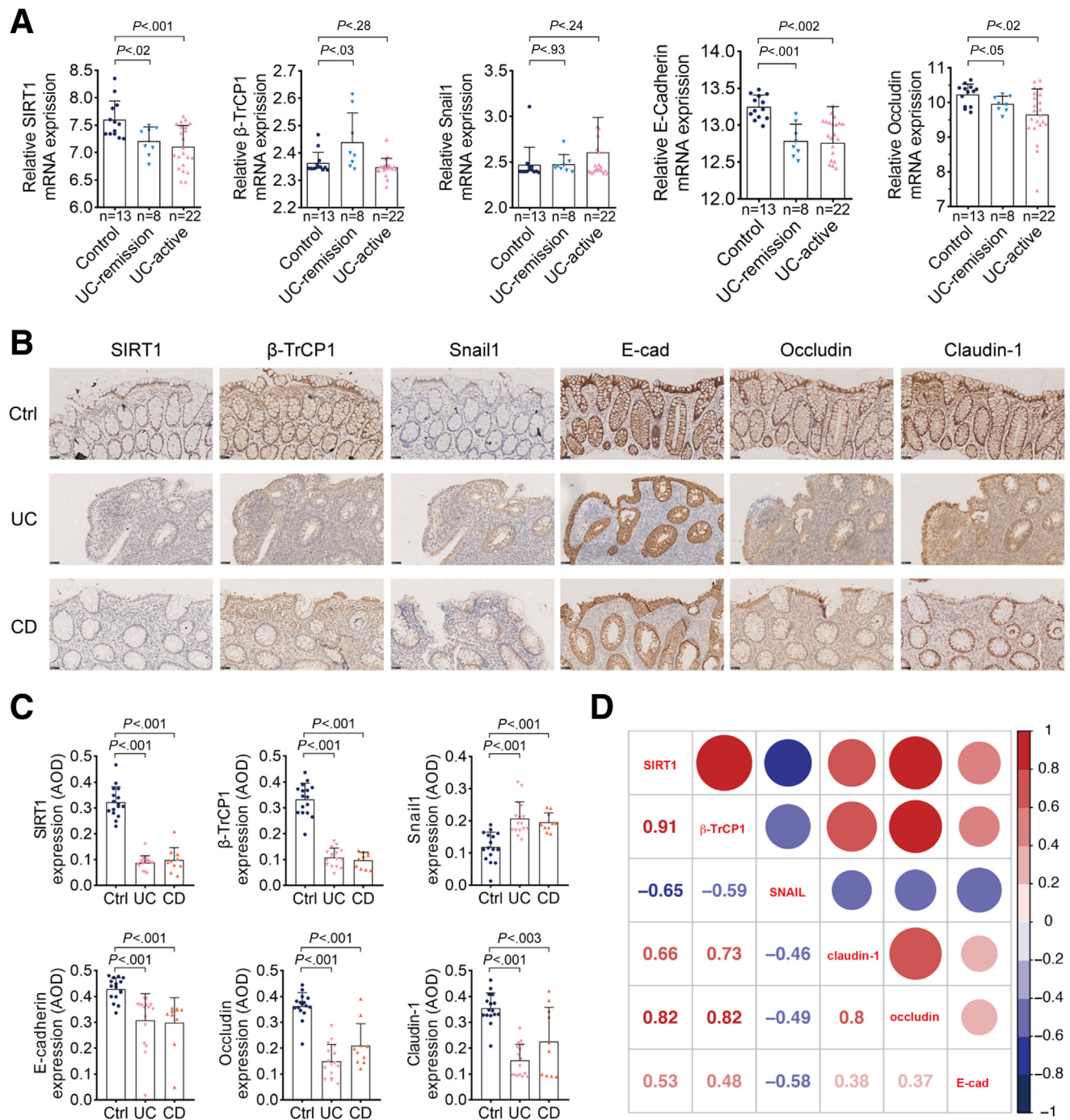


**Figure 6. The SIRT1- $\beta$ -TrCP1-Snail1 axis is associated with human IBD.** (A) The mRNA expression of the relevant genes from human UC patients was analyzed using the GSE38713 dataset (Control: n = 13; UC-remission: n = 8; UC-active: n = 22). (B) The protein expression of SIRT1,  $\beta$ -TrCP1, Snail1, E-cadherin, Occludin, or Claudin-1 in the colonic epithelium of human IBD patients was examined by immunohistochemistry (Scale bar = 100  $\mu$ m). (C) The quantitative analyses of data derived from B by average optical density (AOD) was performed (Control: n = 12; UC: n = 12; CD: n = 10). Data were presented as mean  $\pm$  standard error of the mean. Comparisons were performed with 2-way analysis of variance with Tukey test (A and B). (D) A Pearson correlation chart shows the relationship of paired protein expression using data derived from B.

underscoring the urgency of identifying safer and more efficacious therapeutic options. Recent preclinical investigations reveal that NMN exerts beneficial effects across diverse diseases.<sup>47</sup> In this study, we found that NMN treatment significantly mitigates the DSS-induced reduction

of SIRT1 deacetylase activity, leading to an improvement in the function of the epithelial barrier and subsequent amelioration of DSS-induced colitis in mice, suggesting that NMN may exert a beneficial effect in IBD by activating SIRT1 in enhancing the integrity of the intestinal epithelial barrier.



## Materials and Methods

### Antibodies and Reagents

Antibody for SIRT1 (17-307) was purchased from Upstate Biotechnology (Lake Placid, NY). Antibody for  $\beta$ -TrCP1 (DF6534), FBXL14 (DF13005), Occludin (DF7504), and Claudin-1 (AF0127) were purchased from Affinity Biosciences LTD (Jiangsu, China). Antibody for Snail1 (sc-271977) was purchased from Santa Cruz Biotechnology (CA). Antibodies for E-cadherin (ab-40772), Actin (ab-0033), and GAPDH (ab-0037) were purchased from Abcam (Cambridge, MA). DSS (40 kDa) was purchased from Aladdin Reagent INC (Shanghai, China). FITC-Dextran (FD4, 4 kDa) was purchased from Sigma-Aldrich (St. Louis, MO). NMN was purchased from Selleck (Houston, TX).

### Clinical Specimens

Colon clinical specimens were obtained from patients diagnosed with IBD and non-IBD individuals (serving as control subjects) during endoscopic procedures. The procurement and use of these human colon specimens received approval from the Ethics Committee on Biomedical Research at West China Hospital of Sichuan University (Ethics Approval Number: 2021-508). Histologic analysis was used to confirm the diagnosis of each specimen.

### Microarray Data

The gene expression dataset GSE9452<sup>62</sup> and GSE38713<sup>63</sup> were obtained from the NCBI Gene Expression Omnibus database, which is based on a GPL570 (HG-U133\_Plus\_2) Affymetrix Human Genome U133 Plus 2.0 Array platform. A total of 26 samples are included in the GSE9452 dataset, including 5 non-IBD control subjects and 21 UC samples. A total of 43 samples are included in the GSE38713 dataset, including 13 healthy control subjects, 8 inactive UC samples, and 23 active UC samples.

### Mouse Models

According to DiGiovanni's methods,<sup>64</sup> we constructed BK5.mSIRT1 transgenic mice abbreviated SIRT1-TG mice supported by Cyagen biosciences INC (Guangzhou, China).

All mice were in a C57BL/6 background and kept in standard, infection-free housing conditions, with 12 hour light/dark cycles and 3–5 mice per cage. There was strictly pathogen-free quality of the mouse colonies. All research completed in the manuscript was performed under the guidance of the Northwestern University Institutional Animal Care and Use Committee. Primers for genotyping SIRT1-TG mice are listed as follows: forward primer (5'-3'): CAG-GAAGACAGCGTTTGCACC, and reverse primer (5'-3'): CAAACTCACCTGAAGTTCTCAAGC.

### Induction, Intervention, and Clinical Evaluation of DSS Colitis

Four-month-old sex-matched cohoused mice were administered 3% DSS (40 kDa, Aladdin reagent INC, Shanghai, China) in their drinking water (normal drinking as a negative control) ad libitum for 8 consecutive days,

followed by 1 day of normal drinking water for generating acute colitis model. The NMN groups were administered daily with NMN (0.3 mg/g bodyweight/day) by intraperitoneal injection during DSS treatment to intervene in disease development. Clinical parameters, such as weight loss and rectal bleeding, were monitored daily. The appearance of blood in the stool was measured by fecal occult blood reagent (BASO Diagnostics INC, Zhuhai, China). The severity of rectal bleeding was given a score from 0 to 4, defined as follows: 0 for no color reaction, 1 for color reaction appeared within 1~2 minutes, 2 for color reaction appeared within 1 minute, 3 for color reaction appeared within 10 seconds, and 4 for color reaction was appeared at once. Postmortem, the entire colon was removed from the caecum to the anus, and the colon length was measured. Spleens were collected and weighed. Blood was centrifuged in 3500 *g* for 15 minutes at 4°C to isolate serum. All tissues were stored at -80°C for further use.

### Intestinal Permeability In Vivo and Intercellular Permeability In Vitro

For the in vivo intestinal permeability assay, all mice were fasted for 8 hours and then gavage with FD4 at a concentration of 0.6 mg/g body weight. Plasma samples were collected 4 hours later. For the in vitro intercellular permeability assay, a total of  $1 \times 10^5$  cells were seeded in 24-well Transwell chambers (6.4 mm diameter, 8  $\mu$ m pore size, FALCON) and cultured to the formation of the cell monolayer. After 4% DSS treated cells 8 hour, 1 mg/mL FD4 was added to the upper chamber and medium from the basolateral chamber was collected 2 hours later. The fluorescence intensity of 100  $\mu$ L serum or medium was measured using a fluorescence spectrophotometer (485 nm excitation and 535 nm emission). FD4 concentration was obtained from curves generated by FD4 dilution.

### Quantitative Real-Time PCR

Total RNA from cells was isolated using the innuPREP RNA Mini Kit (Analytik, Jena, Germany) and total RNA from colon was isolated using Trizol (Invitrogen). cDNA was prepared with ReverTra Ace qPCR RT Master Mix (TOYOBO, Osaka, Japan) and analyzed by real-time PCR system (Applied Biosystems, CA) using the QuantiTect SYBR Green PCR Kit (Qiagen, Hilden, Germany) according to the manufacturer's instructions. Sequences of specific primers used for qPCR are listed in Table 1.

### Enzyme-Linked Immunosorbent Assay Analysis

The protein levels of the inflammatory factor interleukin-6 derived from mice serum samples were determined using the mouse interleukin-6 enzyme-linked immunosorbent assay kits (Solarbio Science & Technology, Beijing, China), according to the manufacturer's protocol.

### Histology and Immunohistochemistry

Colon tissues were fixed overnight in 4% paraformaldehyde, embedded in paraffin, sectioned, and stained

**Table 1.** List of Primer Sequences

Gene	Forward 5'-3'	Reverse 5'-3'
<i>mSIRT1</i>	TTGGAAGATGATACGGAGAGG	GCCATCACCACCTTTGTACAAG
<i>hSIRT1</i>	TTGGAAGATGATACGGAGAGG	GCCATCACCACCTTTGTACAAG
<i>hBTRC</i>	GGACACAAACGAGGCATTGCCT	CAACGCACCAATTCCTCATGGC
<i>hSNAI1</i>	GGCCCTGGCTGCTACAAGGC	CTCGAGGGTCAGCGGGGACA
<i>hCDH1</i>	GGATGTGCTGGATGTGAATG	CACATCAGACAGGATCAGCAGAA
<i>hOCLN</i>	GATGAGCAGCCCCCAAT	GGTGAAGGCACGTCCTGTGT
<i>hCLDN1</i>	CAGTCAATGCCAGGTACGAATTT	AAGTAGGGCACCTCCCAGAAG
<i>mIl6</i>	CGGAGAGGAGACTTCACAGAG	ATTTCCACGATTTCCAGAG
<i>mTnf</i>	AGGCACTCCCCCAAAGAT	CAGTAGACAGAAGAGCGTGGTG
<i>hGAPDH</i>	GGGGAGCCAAAAGGGTCATCATCT	GAGGGGCCATCCACAGTCTTCT
<i>mActb</i>	CTGAATGGCCAGGTCTGA	CCCTGGCTGCCTCAACAC

with hematoxylin and eosin for histology analysis. Sections were deparaffinized in xylene and rehydrated through a graded ethanol series. Then, they were antigen retrieved, quenched of endogenous peroxidase, and incubated with indicated primary antibodies overnight at 4°C. After washing with phosphate-buffered saline (PBS) 3 times, tissues were incubated with a second antibody (Beyotime Biotechnology, Shanghai, China), developed with the DAB reagent and counterstained with hematoxylin.<sup>65</sup> The expression of indicated proteins was quantified by average optical density analysis.

### Cell Culture and Drug Treatment

Human colorectal adenocarcinoma Caco2 cells were maintained in Dulbecco's modified Eagle's medium (DMEM, Hyclone, Logan, UT) supplemented with 20% fetal bovine serum (Hyclone). Human colorectal carcinoma HCT116 cells and human kidney HEK-293T cells were maintained in DMEM supplemented with 10% fetal bovine serum. All cells were grown in media containing 100 U penicillin-G/streptomycin sulfate at 37°C in a humidified incubator under 5% CO<sub>2</sub>.

DSS (indicated concentration) treated Caco2, HCT116, or stale cells for 8 hours, and then cells were collected for further studies. Before a DSS treatment, NMN (indicated concentration) treated Caco2 or stale cells for 48 hours or indicated time, and then cells were collected for further studies.

### Plasmids and Lentivirus Infection

Recombinant plasmids, pLVX-puro-SIRT1, pLKO.1-puro-shSIRT1-#1~#3 or pLKO.1-puro-shSnail1-#1~#2 (Target sequences of shRNAs are listed in Table 2), was cotransfected with packaging plasmids pMD2G and psPAX2 into HEK-293T cells for 48 hours, followed by culture medium collection and ultracentrifugation at 25,000 *g* for 2 hours. Pellets were resuspended in DMEM medium and viral titers were determined by infecting HEK293T cells with diluted viruses. Cells were incubated with lentiviruses in the presence of 10  $\mu$ g/mL polybrene and were cultured for 24 hours

to allow target proteins expression, followed by sorting of positive cells through 1  $\mu$ g/mL puromycin treatment for 48 hours.

### Crypt Isolation, Colonic Organoid Culture, and Immunofluorescence

Mouse colonic crypts were isolated as previously described.<sup>66</sup> In brief, the mouse colon was flushed with cold PBS and opened longitudinally, and mucus was removed. The intestine was cut into small fragments and incubated with 5 mM EDTA in PBS on ice for 30 minutes. Epithelium was detached by vigorous shaking. To enrich crypts, tissue suspension was filtered through 100- $\mu$ m sterile cell strainer. Enriched crypts were washed once with cold PBS. About 500 crypts were suspended in 20  $\mu$ L Matrigel (#354230, Corning) supplemented with lentivirus (10<sup>7</sup> PFU). Then, a 20- $\mu$ L droplet of Matrigel/crypts mix was put in the center of a well in a 24-well plate for 15 minutes at 37°C, 500  $\mu$ L of Colon organoid medium (JFKR-MNC-100-KIT, Shanghai JFKR Organoid Biotechnology Co, Ltd) was overlain. The

**Table 2.** List of shRNA Sequences

shRNAs	Sequences (5'-3')
shRNA specific for GFP	GAAGCAGCACGACTTCTTC
shRNA-1 specific for human <i>SIRT1</i>	GAAGTGCTCAGATATTAA
shRNA-2 specific for human <i>SIRT1</i>	GTTGACCTCCTCATTGTTA
shRNA-3 specific for human <i>SIRT1</i>	GCAAAGCCTTTCTGAATCTAT
shRNA-1 specific for human <i>SNAI1</i>	CCACTCAGATGTCAAGAAGTA
shRNA-2 specific for human <i>SNAI1</i>	CCAGGCTCGAAAGGCCCTTCAA
shRNA-1 specific for mouse <i>Sirt1</i>	GAGGGTAATCAATACCTGTTT
shRNA-2 specific for mouse <i>Sirt1</i>	CCTGAAAGAACTGTACCACAA
shRNA-1 specific for mouse <i>Snai1</i>	ATGTGTCTCCCAAGTATTTT
shRNA-2 specific for mouse <i>Snai1</i>	GCCACCTTCTTTGAGGTACAA

medium was changed every 2 days. On the eighth day, the organoids were fixed in 4% paraformaldehyde 30 minutes at room temperature, dehydrated by 30% sucrose overnight at 4°C, embedded in O.C.T., and sectioned. To perform immunofluorescence staining, the sections were permeabilized with 0.3% Triton X-100 in PBS for 15 minutes. After blocking with 4% bovine serum albumin in PBS for 1 hour, the sections were incubated overnight at 4°C with antibodies, diluted in a 4% bovine serum albumin in PBS solution. After washing 3 times with PBS, the sections were incubated with secondary antibodies for 1 hour and cell nuclei were counterstained with DAPI for 10 minutes. Images were acquired using Confocal Microscope. The expression of indicated proteins was quantified by average optical density analysis using QuPath 0.4.1.

### *SIRT1 Deacetylase Activity Assay*

For SIRT1 deacetylase activity assay, samples were subjected to Fluor de LysSIRT1 assay. Briefly, cell lysates were subjected to immunoprecipitation by an antibody specific for SIRT1 (07-131; Upstate Biotechnology), and then captured with agarose-conjugated protein A beads. Resuspended samples were added to a reaction mixture containing Ac-p53-fluorogenic-substrate (AK-555; Biomol Research Laboratories, Plymouth Meeting, PA), and incubated at room temperature. After 1 hour, developer is added to stop reaction, and then incubated on 37°C for 1 hour. The fluorescence is measured.

### *Western Blotting*

Total protein was extracted with cold EBC250 lysis buffer, protease inhibitor, and phosphatase inhibitor cocktail. Equal amounts of proteins were separated by 10% sodium dodecyl sulfate polyacrylamide gels and then transferred to a PVDF membrane that was blocked with 5% skim milk prepared in tris-buffered saline with Tween. Then, the membrane was incubated with indicated primary antibodies overnight at 4°C. Following washes in tris-buffered saline with Tween, the membrane was subsequently incubated with the appropriate horseradish peroxidase-conjugated secondary antibodies for 1 hour and then visualized via enhanced chemiluminescence detection. Protein expression was quantified by densitometric analysis using ImageJ software (National Institutes of Health, Bethesda, MD).

### *Half-life Analyses*

CHX (25 µg/mL) treated cells for the indicated time, and then cell lysates were subjected to Western blotting. Protein expression was quantified by densitometric analysis using ImageJ software.

### *Statistical Analysis*

Unpaired 2-sided Student *t* tests were used for analyses that involved only 2 groups for comparison, and analysis of variance tests were used for analyses that involved more than 2 groups for comparison. All data shown represent the

means ± standard error of the mean, and statistically significant differences are indicated as follows: \**P* < .05; \*\**P* < .01; \*\*\**P* < .001.

## References

1. Agrawal M, Allin K, Petralia F, et al. Multiomics to elucidate inflammatory bowel disease risk factors and pathways. *Nat Rev Gastroenterol Hepatol* 2022;19:399–409.
2. Ahmed S, Alam S, Alsabri M. Health-related quality of life in pediatric inflammatory bowel disease patients: a narrative review. *Cureus* 2022;14:e29282.
3. Silva LC, Seixas R, de Carvalho E. Quality of life in children and adolescents with inflammatory bowel disease: impact and predictive factors. *Pediatr Gastroenterol Hepatol Nutr* 2020;23:286–296.
4. Zeng Z, Jiang M, Li X, et al. Precision medicine in inflammatory bowel disease. *Precis Clin Med* 2023;6:pbad033.
5. Shah SC, Itzkowitz SH. Colorectal cancer in inflammatory bowel disease: mechanisms and management. *Gastroenterology* 2022;162:715–730.e713.
6. Lutgens W, Martijn G, Geert J, et al. Declining risk of colorectal cancer in inflammatory bowel disease: an updated meta-analysis of population-based cohort studies. *Inflamm Bowel Dis* 2013;19:789–799.
7. Keller DS, Windsor A, Cohen R, et al. Colorectal cancer in inflammatory bowel disease: review of the evidence. *Tech Coloproctol* 2019;23:3–13.
8. Di Tommaso N, Gasbarrini A, Ponziani FR. Intestinal barrier in human health and disease. *Int J Environ Res Public Health* 2021;18:12836.
9. Seo K, Seo J, Yeun J, et al. The role of mucosal barriers in human gut health. *Arch Pharm Res* 2021;44:325–341.
10. Horowitz A, Chanez-Paredes SD, Haest X, et al. Paracellular permeability and tight junction regulation in gut health and disease. *Nat Rev Gastroenterol Hepatol* 2023;20:417–432.
11. Mishra SP, Wang B, Jain S, et al. A mechanism by which gut microbiota elevates permeability and inflammation in obese/diabetic mice and human gut. *Gut* 2023;72:1848–1865.
12. Farre R, Fiorani M, Abdu Rahiman S, et al. Intestinal permeability, inflammation and the role of nutrients. *Nutrients* 2020;12:1185.
13. Parikh K, Antanaviciute A, Fawcner-Corbett D, et al. Colonic epithelial cell diversity in health and inflammatory bowel disease. *Nature* 2019;567:49–55.
14. Ivanov AI, Nusrat A, Parkos CA. The epithelium in inflammatory bowel disease: potential role of endocytosis of junctional proteins in barrier disruption. *Novartis Found Symp* 2004;263:115–124; discussion 124–132, 211–118.
15. Mehta S, Nijhuis A, Kumagai T, et al. Defects in the adherens junction complex (E-cadherin/ beta-catenin) in inflammatory bowel disease. *Cell Tissue Res* 2015;360:749–760.
16. Nenci A, Becker C, Wullaert A, et al. Epithelial NEMO links innate immunity to chronic intestinal inflammation. *Nature* 2007;446:557–561.



17. Sharma M, Mohapatra J, Wagh A, et al. Involvement of TACE in colon inflammation: a novel mechanism of regulation via SIRT-1 activation. *Cytokine* 2014; 66:30–39.
18. Xu C, Wang L, Fozouni P, et al. SIRT1 is downregulated by autophagy in senescence and ageing. *Nat Cell Biol* 2020;22:1170–1179.
19. Tran D, Bergholz J, Zhang H, et al. Insulin-like growth factor-1 regulates the SIRT1-p53 pathway in cellular senescence. *Aging Cell* 2014;13:669–678.
20. Huang Q, Su H, Qi B, et al. A SIRT1 activator, Ginse-noside Rc, promotes energy metabolism in car-diomyocytes and neurons. *J Am Chem Soc* 2021; 143:1416–1427.
21. Zhang Y, Li T, Pan M, et al. SIRT1 prevents cigarette smoking-induced lung fibroblasts activation by regu-lating mitochondrial oxidative stress and lipid meta-bolism. *J Transl Med* 2022;20:222.
22. Xu K, Yang Y, Lan M, et al. Apigenin alleviates oxida-tive stress-induced myocardial injury by regulating SIRT1 signaling pathway. *Eur J Pharmacol* 2023; 944:175584.
23. Singh V, Ubaid S. Role of Silent Information Regulator 1 (SIRT1) in regulating oxidative stress and inflammation. *Inflammation* 2020;43:1589–1598.
24. He S, Wang Y, Liu J, et al. Activating SIRT1 deacetylates NF-kappaB p65 to alleviate liver inflammation and fibrosis via inhibiting NLRP3 pathway in macrophages. *Int J Med Sci* 2023;20:505–519.
25. Zhao Q, Tian Z, Zhou G, et al. SIRT1-dependent mito-chondrial biogenesis supports therapeutic effects of resveratrol against neurodevelopment damage by fluo-ride. *Theranostics* 2020;10:4822–4838.
26. He F, Li Q, Sheng B, et al. SIRT1 inhibits apoptosis by promoting autophagic flux in human nucleus pulposus cells in the key stage of degeneration via ERK signal pathway. *Biomed Res Int* 2021;2021:8818713.
27. Yan D, Yang Y, Lang J, et al. SIRT1/FOXO3-mediated autophagy signaling involved in manganese-induced neuroinflammation in microglia. *Ecotoxicol Environ Saf* 2023;256:114872.
28. Baeken MW. Sirtuins and their influence on autophagy. *J Cell Biochem* Published online February 6, 2023. <https://doi.org/10.1002/jcb.30377>.
29. Shen P, Deng X, Chen Z, et al. SIRT1: a potential ther-apeutic target in autoimmune diseases. *Front Immunol* 2021;12:779177.
30. Devi K, Singh N, Jaggi AS. Dual role of sirtuin 1 in in-flammatory bowel disease. *Immunopharmacol Immuno-toxicol* 2020;42:385–391.
31. Wellman AS, Metukuri MR, Kazgan N, et al. Intestinal Epithelial Sirtuin 1 regulates intestinal inflammation dur-ing aging in mice by altering the intestinal microbiota. *Gastroenterology* 2017;153:772–786.
32. Ren MT, Gu ML, Zhou XX, et al. Sirtuin 1 alleviates endoplasmic reticulum stress-mediated apoptosis of in-testinal epithelial cells in ulcerative colitis. *World J Gas-troenterol* 2019;25:5800–5813.
33. Sun H, Cai H, Fu Y, et al. The protection effect of resveratrol against radiation-induced inflammatory bowel disease via NLRP-3 inflammasome repression in mice. *Dose Response* 2020;18:1559325820931292.
34. Caruso R, Marafini I, Franzè E, et al. Defective expression of SIRT1 contributes to sustain inflammatory pathways in the gut. *Mucosal Immunol* 2014;7:1467–1479.
35. Liu W, Ruan T, Ji X, et al. The Gli1-Snail axis contributes to *Salmonella typhimurium*-induced disruption of intercellular junctions of intestinal epithelial cells. *Cell Microbiol* 2020; 22:e13211.
36. Ohkubo T, Ozawa M. The transcription factor Snail downregulates the tight junction components indepen-dently of E-cadherin downregulation. *J Cell Sci* 2004; 117:1675–1685.
37. Wang Y, Shi J, Chai K, et al. The role of Snail in EMT and tumorigenesis. *Curr Cancer Drug Targets* 2013; 13:963–972.
38. Wu Y, Zhou BP. Snail: More than EMT. *Cell Adh Migr* 2010;4:199–203.
39. Badarinath K, Dam B, Kataria S, et al. Snail maintains the stem/progenitor state of skin epithelial cells and carci-nomas through the autocrine effect of matricellular pro-tein Mindin. *Cell Rep* 2022;40:111390.
40. Zidar N, Bostjancic E, Jerala M, et al. Down-regulation of microRNAs of the miR-200 family and up-regulation of Snail and Slug in inflammatory bowel diseases: hallmark of epithelial-mesenchymal transition. *J Cell Mol Med* 2016;20:1813–1820.
41. Lakhan SE, Kirchgessner A. Gut microbiota and sirtuins in obesity-related inflammation and bowel dysfunction. *J Transl Med* 2011;9:1–12.
42. Yu Q, Zhou BP, Wu Y. The regulation of snail: on the ubiquitin edge. *Cancer Cell Microenviron* 2017;4:e1567.
43. Zhou BP, Deng J, Xia W, et al. Dual regulation of Snail by GSK-3beta-mediated phosphorylation in control of epithe-lial-mesenchymal transition. *Nat Cell Biol* 2004;6:931–940.
44. Dang F, Jiang C, Zhang T, et al. PCAF and SIRT1 modu-late betaTrCP1 protein stability in an acetylation-dependent manner. *J Genet Genomics* 2021;48:652–655.
45. Yoshino J, Baur JA, Imai SI. NAD(+) intermediates: the biology and therapeutic potential of NMN and NR. *Cell Metab* 2018;27:513–528.
46. Imai S. A possibility of nutraceuticals as an anti-aging intervention: activation of sirtuins by promoting mamma-lian NAD biosynthesis. *Pharmacol Res* 2010;62:42–47.
47. Hong W, Mo F, Zhang Z, et al. Nicotinamide mono-nucleotide: a promising molecule for therapy of diverse diseases by targeting NAD+ metabolism. *Front Cell Dev Biol* 2020;8:246.
48. Lo Sasso G, Ryu D, Mouchiroud L, et al. Loss of Sirt1 function improves intestinal anti-bacterial defense and protects from colitis-induced colorectal cancer. *PLoS One* 2014;9:e102495.
49. Melhem H, Hansmann F, Bressenot A, et al. Methyl-deficient diet promotes colitis and SIRT1-mediated endoplasmic reticulum stress. *Gut* 2016;65:595–606.
50. Singh UP, Singh NP, Singh B, et al. Resveratrol (trans-3, 5, 4'-trihydroxystilbene) induces silent mating type information regulation-1 and down-regulates nuclear transcription fac-tor- $\kappa$ B activation to abrogate dextran sulfate sodium-induced colitis. *J Pharmacol Exp Ther* 2010;332:829–839.

51. Huang P, Wang X, Wang S, et al. Treatment of inflammatory bowel disease: potential effect of NMN on intestinal barrier and gut microbiota. *Curr Res Food Sci* 2022;5:1403–1411.
52. Kuo W-T, Shen L, Zuo L, et al. Inflammation-induced occludin downregulation limits epithelial apoptosis by suppressing caspase-3 expression. *Gastroenterology* 2019;157:1323–1337.
53. Pope JL, Bhat AA, Sharma A, et al. Claudin-1 regulates intestinal epithelial homeostasis through the modulation of Notch-signalling. *Gut* 2014;63:622–634.
54. Wheeler JMD, Kim HC, Efstathiou JA, et al. Hypermethylation of the promoter region of the E-cadherin gene (CDH1) in sporadic and ulcerative colitis associated colorectal cancer. *Gut* 2001;48:367–371.
55. Chiang C, Ayyanathan K. Snail/Gfi-1 (SNAG) family zinc finger proteins in transcription regulation, chromatin dynamics, cell signaling, development, and disease. *Cytokine Growth Factor Rev* 2013;24:123–131.
56. Díaz VM, de Herreros AG. F-box proteins: keeping the epithelial-to-mesenchymal transition (EMT) in check. *Semin Cancer Biol* 2016;36:71–79.
57. Woo SR, Byun JG, Kim YH, et al. SIRT1 suppresses cellular accumulation of  $\beta$ -TrCP E3 ligase via protein degradation. *Biochem Biophys Res Commun* 2013;441:831–837.
58. Zhang C, Zeng F, Fan Z, et al. An oral polyphenol host-guest nanoparticle for targeted therapy of inflammatory bowel disease. *Acta Biomater* 2023;10:5009.
59. Nakase H, Uchino M, Shinzaki S, et al. Evidence-based clinical practice guidelines for inflammatory bowel disease 2020. *J Gastroenterol* 2021;56:489–526.
60. Troskot B, Simunic M. [Side effects and contraindications for biological therapy in inflammatory bowel disease]. *Acta Med Croatica* 2013;67:131–143.
61. Bruscoli S, Febo M, Riccardi C, et al. Glucocorticoid therapy in inflammatory bowel disease: mechanisms and clinical practice. *Front Immunol* 2021;12:691480.
62. Olsen J, Gerds TA, Seidelin JB, et al. Diagnosis of ulcerative colitis before onset of inflammation by multivariate modeling of genome-wide gene expression data. *Inflamm Bowel Dis* 2009;15:1032–1038.
63. Planell N, Lozano JJ, Mora-Buch R, et al. Transcriptional analysis of the intestinal mucosa of patients with ulcerative colitis in remission reveals lasting epithelial cell alterations. *Gut* 2013;62:967–976.
64. DiGiovanni J, Bol DK, Wilker E, et al. Constitutive expression of insulin-like growth factor-1 in epidermal basal cells of transgenic mice leads to spontaneous tumor promotion. *Cancer Res* 2000;60:1561–1570.
65. Sun S, Yi Y, Xiao Z-XJ, et al. ER stress activates TAp73 $\alpha$  to promote colon cancer cell apoptosis via the PERK-ATF4 pathway. *J Cancer* 2023;14:1946–1955.
66. Sato T, Stange DE, Ferrante M, et al. Long-term expansion of epithelial organoids from human colon, adenoma, adenocarcinoma, and Barrett's epithelium. *Gastroenterology* 2011;141:1762–1772.

---

Received October 30, 2023. Accepted May 3, 2024.

#### Correspondence

Address correspondence to: Yang Wang, PhD, Sichuan University, No. 24 South Section 1, Yihuan Road, Chengdu 610065, China. e-mail: wangy90@scu.edu.cn; or Zhi-Xiong Jim Xiao, PhD, Sichuan University, No. 24 South Section 1, Yihuan Road, Chengdu 610065, China. e-mail: jimzx@scu.edu.cn; or Hu Zhang, PhD, Sichuan University, No. 37 Guoxue Lane, Wuhou District, Chengdu 610041, China. e-mail: tigerwucms03@sina.com.

#### Acknowledgments

We thank members of the Z.-X.J.X. laboratory for stimulating discussions during this study and Mr. Han Kang for help on instruments.

#### CRedit Authorship Contributions

Liang Wang, PhD (Conceptualization: Equal; Data curation: Lead; Formal analysis: Lead; Funding acquisition: Equal; Writing – original draft: Equal)  
 Jinsong Li, Bachelor (Data curation: Equal)  
 Mingshan Jiang, PhD (Resources: Equal)  
 Yue Luo, Bachelor (Data curation: Supporting)  
 Xiaoke Xu, Bachelor (Data curation: Supporting)  
 Juan Li, PhD (Data curation: Supporting)  
 Yang Pan, MD (Data curation: Supporting)  
 Hu Zhang, PhD (Conceptualization: Equal)  
 Zhi-Xiong Jim Xiao, PhD (Conceptualization: Lead; Funding acquisition: Equal; Writing – review & editing: Lead)  
 Yang Wang, PhD (Data curation: Supporting; Funding acquisition: Equal; Methodology: Lead; Writing – original draft: Lead)

#### Conflicts of interest

The authors disclose no conflicts.

#### Funding

This work was supported by the National Key R&D Program of China (2022YFA1103701 to Z.-X.J.X.), National Natural Science Foundation of China (81830108 to Z.-X.J.X., and 82103167 to Y.W.), Natural Science Foundation of Sichuan Province for Youth Scholars (2023NSFSC1612 to L.W.), the City-School Science and Technology Strategic Cooperation Project of Nanchong City (22SXZRKX0011 to L.W.), the Doctoral Initiation Fund of North Sichuan Medical College (CBY22-QDA16 to L.W.), Fundamental Research Funds for the Central Universities (2023SCU12109 to Y.W.), China Postdoctoral Science Foundation (2021M702363 to Y.W.), Sichuan Science and Technology Program (2023YFS0279, 2023YFS0287, 2021YFH0189 to H.Z.), Sichuan Ganbao Program (GBKT22013 to H.Z.), and West China Clinical research Incubation Program (2021HXFH065 to H.Z.).